https://doi.org/10.5194/amt-2021-337
Preprint. Discussion started: 21 October 2021

Atmospheric Measurement Techniques Discussions

Intercomparison of Vaisala RS92 and RS41 radiosonde temperature sensors under controlled laboratory conditions

Marco Rosoldi[1,*], Graziano Coppa[2,*], Andrea Merlone[2], Chiara Musacchio[2], Fabio Madonna[1]

[1] Consiglio Nazionale delle Ricerche - Istituto di Metodologie per l'Analisi Ambientale (CNR-IMAA), Tito Scalo, Italy
[2] Istituto Nazionale di Ricerca Metrologica (INRiM), Torino, Italy
*These authors contributed equally to this work.

Correspondence to: Marco Rosoldi (marco.rosoldi@imaa.cnr.it) and Graziano Coppa (g.coppa@inrim.it)

Abstract. Radiosounding profiles are essential for weather and climate applications, as well as for the calibration and validation of remote sensing measurements. Vaisala RS92 radiosondes have been widely used on a global scale until 2016, although in the fall of 2013 Vaisala introduced the RS41 model to progressively replace the RS92. To ensure homogeneity and the highest quality of data records following the transition from RS92 to RS41, intercomparisons of the two radiosonde models are needed. An intercomparison experiment has been performed where, for the first time and independently of the manufacturer, RS92 and RS41 radiosondes have been simultaneously tested and compared inside climatic chambers in order to characterize the noise, the calibration accuracy and the bias of their temperature measurements. A pair of RS41 and RS92 radiosondes has been tested at ambient pressure under very different temperature and humidity conditions. The results reveal that the temperature sensor of RS41 is less affected by noise and more accurate than that of RS92, with noise values less than 0.06 °C for RS41 and less than 0.1 °C for RS92. The error corrected by means of calibration, evaluated as the deviation from a reference value and referred as calibration error, is within ±0.1 °C for RS41 and the related uncertainty (hereafter with coverage factor k =1) is less than 0.06 °C, while RS92 is affected by a cold bias in the calibration, which ranges from 0.1 °C up to a few tenths of a degree, with a calibration uncertainty less than 0.1 °C. Under conditions similar to those that radiosondes meet at the ground in nighttime radiosoundings, the temperature bias between RS41 and RS92 is within ±0.1 °C, while its uncertainty is less than 0.1°C. The radiosondes have also been tested before and after fast (within ≈ 10 s) temperature changes of about ±20 °C, simulating a scenario similar to steep thermal changes that radiosondes may meet when passing from indoor to outdoor environment during the pre-launch phase. The results reveal that such thermal changes may increase the noise of temperature sensors during radiosoundings, up to 0.1 °C for the RS41 and up to 0.3 °C for the RS92, with a similar increase in the calibration uncertainty of temperature sensors, as well as an increase in the uncertainty of their bias up to 0.3 °C. However, the thermal changes do not appear to affect sensors' calibration error and temperature bias.

1 Introduction

Atmospheric profiles of temperature, humidity and wind (speed and direction) measured with radiosoundings are essential for a wide variety of scientific applications, such as the study of the atmospheric thermodynamic structure and related processes (e.g., Seidel et al., 2010; Rapp et al., 2011), the analysis of trends to detect and monitor signals of

https://doi.org/10.5194/amt-2021-337
Preprint. Discussion started: 21 October 2021

Atmospheric Measurement Techniques Discussions

climate change both in troposphere and stratosphere (e.g., Gaffen et al., 2000; Free et al., 2005; McCarthy, 2008; Sherwood et al., 2008; McCarthy et al., 2009; Thorne et al., 2011; Philipona et al., 2018; SY et al., 2020; Madonna et al., 2021a), the calibration and validation of ground-based and satellite remote sensing measurements (e.g., Whiteman et al., 1992; Zhou et al., 2007; Pougatchevet al., 2009; Loew et al., 2017; Finazzi et al., 2019), the improvement of weather forecasting, climate models and atmospheric reanalysis (e.g., Haimberger et al., 2012; Hersbach et al., 2018, 2020).

Vaisala RS92 radiosondes, introduced in 2003, have been mostly used on a global scale until 2016 (Madonna et al., 2021b). In particular, within the Global Climate Observing System (GCOS) Reference Upper-Air Network (GRUAN, Bodeker et al., 2016; http://www.gruan.org), these radiosondes have been adopted by the majority of sites to provide reference measurements, i.e. traceable to SI or community accepted reference standard and with a comprehensive uncertainty analysis and quantification (Dirksen et al., 2014; Thorne et al., 2017). To improve measurement accuracy, in the fall of 2013 Vaisala introduced the RS41 radiosonde to progressively replace the RS92, whose production was terminated late in 2017, although some time is clearly needed to have the majority of global radiosouding stations operating the new RS41 at the same time. Sensors' changes typically lead to inhomogeneities in data records, which may systematically alter the climate signal contained in the data and potentially affect radiosounding historical time series and associated applications and analysis, as demonstrated by several studies (Gaffen, 1994; Parker and Cox, 1995; Lanzante, 1996; Sherwood et al., 2005, 2015; Haimberger et al., 2008, 2012; Madonna et al., 2021b). Intercomparison experiments, such as the last WMO CIMO (World Meteorological Organization Commission for Instruments and Methods of Observation) radiosondes' intercomparison (Nash et al., 2011), are one of the most effective approaches to quantify and adjust these inhomogeneities, as well as to evaluate improvements in sensors' measurement accuracy. Intercomparisons of radiosondes, based on both atmospheric and laboratory measurements, represent a unique opportunity to characterize the differences between their sensors in terms of biases, errors and uncertainty contributions of the measurements.

For the recent transition from RS92 to RS41, the most relevant measurement errors and related uncertainties for both radiosonde models have been characterized through laboratory tests performed by the manufacturer (Vaisala, 2013, 2017a; Jauhiainen et al., 2014; Survo et al., 2014). The evaluated errors include the errors corrected by means of the calibration, evaluated as the difference with respect to traceable reference values and hereafter reported as calibration errors, the radiation errors due to the heating of sensors by solar radiation - which introduces a warm bias in temperature sensors and a dry bias in humidity sensors - and the time lag errors due to the increased response time of sensors at low temperatures, mainly below -40°C (negligible for temperature sensors). Furthermore, additional manufacturer-independent laboratory tests have been performed as part of GRUAN activities for both RS92 (Dirksen et al., 2014) and RS41 (Dirksen et al., 2020; von Rohden et al., 2021).

On the other hand, the difference (bias) between RS92 and RS41measurements has been quantified via dual soundings, i.e., simultaneous atmospheric measurements performed with two radiosondes of different type attached to a payload and lifted by the same balloon. Dual soundings have been performed in different locations and time periods, in order to assess sensors' difference in dependence on regional climate, seasons, daytime and nighttime conditions. Examples are provided both by the manufacturer (Jauhiainen et al., 2014; Vaisala, 2014) and by the GRUAN community (Jensen et al., 2016; Kawai et al., 2017; Sun et al., 2019; Dirksen et al., 2020; Jing et al., 2021). In this regard, starting from 2014, several GRUAN sites have performed dual soundings for periods of different duration and launch frequency, from long-term campaigns (more than one year), typically with weekly or bi-weekly launch frequency, to short intensive campaigns (less than 1 month), typically with daily launch frequency, up to sporadic launches (Dirksen et al., 2020).

In support of the GRUAN intercomparison strategy for managing the transition from RS92 to RS41, only a few dedicated experiments in a laboratory-controlled environment have been carried out. Merging the expertise of the GRUAN station of the CNR-IMAA (National Research Council of Italy - Institute of Methodologies for Environmental Analysis) Atmospheric Observatory (CIAO) and the metrology expertise of the Italian National Institute of Metrology (Istituto Nazionale di Ricerca Metrologica - INRiM), an intercomparison experiment based on laboratory tests has been performed with the aim to characterize RS92 and RS41 performances and differences. More specifically, the noise, the calibration error and the associated uncertainty of radiosondes' temperature sensors, as well as their bias, have been assessed under different controlled temperature and humidity conditions inside climatic chambers, using sensors traceable to SI standards as reference. The methodology and results of this assessment are described and discussed in this paper. This is the first time that, independently of the manufacturer, the RS92 and the RS41 have been simultaneously tested and compared inside climatic chambers in order to characterize the noise, the calibration accuracy and the bias of their temperature measurements.

Comparing radiosondes in climatic chambers has a few advantages compared to dual soundings. First, under controlled measurement conditions in a climatic chamber the bias repeatability can be evaluated, which is not possible in dual soundings, as the atmospheric conditions the two radiosondes meet at each altitude are not precisely the same during each sounding and change in different soundings. Second, for a given measurement scenario, the number of measurements that can be collected in a climatic chamber, even with a single pair of radiosondes, is much larger compared to dual soundings, due to the limited number of dual soundings available for that scenario. Thus, to characterize the bias between the two radiosondes' measurements, a few pairs of radiosondes are sufficient using a climatic chamber, while many more pairs of radiosondes (and higher costs) are required for dual soundings, both to represent a wide variety of measurement scenarios and to collect for each scenario a sufficient number of measurements to minimize the effects on the bias of the different atmospheric conditions that the two radiosondes meet at each altitude level during each sounding. Finally, it is much easier to compare radiosondes of the same production batches in climatic chambers rather than in dual sounding datasets, thus reducing the uncertainty due to the variability of production batches.

In Sect.2., the radiosounding activities at CIAO and the laboratory equipment available at INRiM, where the intercomparison experiment was carried out, are detailed. Section 3 describes the experimental setup and the applied methodology. In Sect. 4, the results of the intercomparison are reported and discussed. Finally, Sect. 5 provides a summary and conclusions.

2 Radiosounding activities at CIAO and laboratory equipment at INRiM

One of the main scientific objectives of CIAO observatory is the long-term observation and study of atmospheric aerosols, water vapor, clouds and their interactions and role in the climate system (Madonna et al., 2011a; http://www.ciao.imaa.cnr.it). Since 2004, launches of Vaisala radiosondes are performed at CIAO with the aim to monitor atmospheric thermodynamic parameters, calibrate a ground-based Raman lidar for the retrieval of atmospheric humidity profiles (Mona et al., 2007; Rosoldi et al., 2013) and validate satellite observations and retrieval algorithms (Zhou et al., 2007; Madonna et al., 2011b). CIAO became a GRUAN site in 2010 and since then routine weekly nighttime radiosoundings are performed, using the RS92 sondes until December 2016 and the RS41 sondes thereafter. RS92 data have been also used to assess how the redundancy of atmospheric humidity measurements performed using radiosoundings and ground-based remote sensing techniques, such as microwave radiometer and Raman lidar, can reduce the random uncertainties in applications using only one of these measurement techniques (Madonna et al., 2014). Until 2016, RS92 radiosondes have been launched at CIAO using both a manual system and an automatic launcher. The database of automatic launchers operated by CIAO and other GRUAN sites has been recently used to assess the reliability and the technical performance of automatic launchers compared to the most common manual systems (Madonna et al., 2020).

INRiM is the Italian National Metrology Institute, with a deep involvement and leadership of metrology projects and international initiatives dedicated to the investigation of temperature measurements and their uncertainties for meteorology and climate applications, such as the MeteoMet projects of the European Metrology Research Programme (Merlone et al. 2015, Merlone et al. 2018). Besides funded projects, INRiM is also deeply involved in the growing collaboration between the metrology and meteorology and climate communities. Metrologists from INRiM serve as chairs and experts in the WMO expert teams, in the CIPM-BIPM[1] working group on environmental metrology, in the GRUAN working group and other study groups and initiatives.

INRiM's laboratories feature facilities and equipment dedicated to the investigation of uncertainties in the measurements of meteorological and climate parameters, and for the calibration of several types of instruments. Within the present study, two climatic chambers have been used for radiosonde testing. The first one is a Kambic MeteoCal KK-105 (Fig. 1, Merlone et al., 2019), specifically adapted by the manufacturer to address a wide range of environmental temperatures (and beyond, range -40 °C/180 °C) and relative humidities (10 %/98 % in the temperature range 10 °C/95 °C). The chamber has been designed to achieve a temperature stability better than 0.1 °C and a uniformity in the measurement space within 0.3 °C, while for relative humidity the stability is 0.5 %. The second climatic chamber is manufactured by Weiss Technik with a temperature stability of 0.2 °C, a uniformity within 0.5 °C and no humidity control capability.

In order to compare the temperature readings from the radiosondes with the reference temperatures inside the climatic chambers, a number of CalPower custom-made reference platinum resistance sensors (Pt100 with metal coating) have been used.

Before their calibration, the Pt100 thermometers were thermally cycled between -20 °C and 50 °C in order to evaluate the repeatability of the instruments. The thermometers were calibrated in a highly stable and homogeneous liquid bath, by comparison with a standard resistance thermometer calibrated at the fixed points of the ITS-90. The thermometers were calibrated at six temperature points: -40 °C, 0 °C, 20 °C, 30 °C, 40 °C and 60 °C, with two hysteresis-check points at 0 °C and 20 °C. The final calibration uncertainty (given here and hereafter with coverage factor k =1, unless specified differently) was evaluated as 0.005 °C for $T > 0$ °C and 0.01 °C for $T < 0$ °C. The reference sensors have been read using a multimeter Fluke 1586A Super DAQ with a multichannel scanner, capable of a measurement uncertainty better than 0.005 °C.

[1] BIPM - Bureau International des Poids et Mesures – International office of weights and measures of the CIPM, the International Committee for weights and measures

https://doi.org/10.5194/amt-2021-337
Preprint. Discussion started: 21 October 2021

Atmospheric Measurement Techniques Discussions

Figure 1: Climatic chamber Kambic MeteoCal KK-105 in operation at INRiM and used to test the performances and differences of RS92 and RS41 under various temperature and humidity conditions and ambient pressure. The chamber simultaneously and independently controls temperature (range -40 °C/180 °C) and relative humidity (range 10 %/98 % in the temperature range 10 °C/95 °C).

3 Experimental setup and methodology

The intercomparison experiment has been carried out by using two separate Vaisala DigiCORA MW41sounding systems (Vaisala, 2018), consisting of a computer and a laptop, running the MW41 sounding software v2.4.0 and v2.6.0 respectively, each connected to its sounding processing subsystem SPS311 (Vaisala, 2016) via a network adapter and to its radiosonde ground check device (Fig. 2). The latter was a GC25 (Vaisala, 2008), connected to the computer via a serial cable, for the RS92, and a RI41 (Vaisala, 2017b), connected to the laptop via a USB cable, for the RS41. Both systems were connected to an omnidirectional ultra-high frequency (UHF) antenna by a splitter and they were configured to separately receive and process the signals transmitted by the two radiosonde models at two different frequencies, 402 MHz for the RS92 and 405 MHz for the RS41, avoiding interference in the received signals.

https://doi.org/10.5194/amt-2021-337
Preprint. Discussion started: 21 October 2021

GC25 and RI41 devices are used in ground check procedures recommended by the manufacturer before radiosondes' launch. In the ground check of RS92 with GC25, humidity sensors are heated with integrated heating elements to remove possible contamination affecting humidity measurements. Moreover, RS92 temperature and humidity measurements are compared to reference values in order to check the factory calibration and determine possible correction factors to be applied to radiosounding temperature and humidity profiles. The reference values for temperature are provided by a Pt100 thermometer located inside the GC25 chamber, while a 0 % humidity reference is obtained using a desiccant in the same chamber. When RS41 is checked with RI41, as for the check of RS92 with GC25, the humidity sensor is heated to remove any residual contamination, using the integrated heating element on the sensor chip. Unlike the check with GC25, RS41 temperature measurements are not compared to reference values and no correction factor to be applied to radiosounding temperature profiles is determined. However, a functionality check of the temperature sensor is performed, by comparing its readings with those of the additional temperature sensor integrated on the humidity sensor chip. Conversely, RS41 humidity measurements are compared to a 0 % humidity reference generated in open air by heating the humidity sensor and taking advantage of the fact that for a given water vapor content, the relative humidity decreases towards zero when the temperature rises enough. This allows to determine a correction factor applicable to radiosounding humidity profiles.

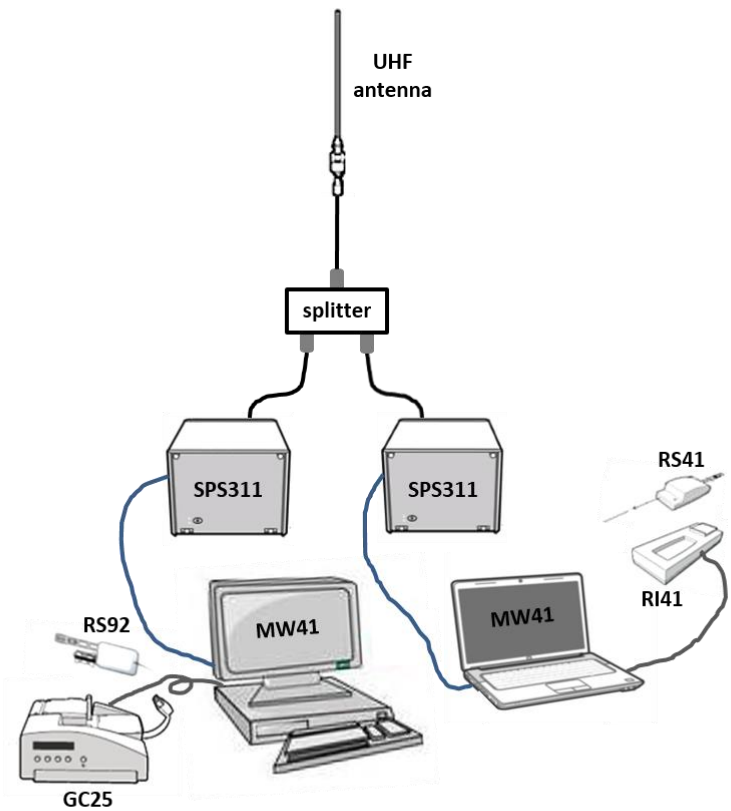

Figure 2: Scheme of Vaisala sounding systems used for the intercomparison, consisting of a computer and a laptop, running the MW41 software, each connected to its sounding processing subsystem (SPS311) and radiosonde ground check device (GC25 for RS92 and RI41 for RS41). Both systems are connected to an omnidirectional ultra-high frequency (UHF) antenna by a splitter.

https://doi.org/10.5194/amt-2021-337
Preprint. Discussion started: 21 October 2021

Atmospheric Measurement Techniques Discussions

In order to simultaneously test both radiosonde types inside a climatic chamber, a customized prototype frame has been used. A light and robust plastic grid was mounted on a metal plate using two cylindrical steel holders fixed both to the metal plate and to the grid with screws and bolts. Two holes have been created on the grid suitable to lodge the sensors' booms of both radiosonde types through two adapters, which are the same used to test radiosondes'sensors in the standard humidity chamber SPRH-100 (Dr. Schulz & Partner GmbH, http://www.drschulz.com) during the manufacturer-independent pre-launch ground-check regularly performed for GRUAN radiosoundings (Immler and al., 2011). The adapters were fixed to the grid with plastic ties and the two radiosondes of different type were kept in a fixed position with their sensor booms vertically oriented opposite each other at a distance of about 15 cm. Both radiosonde types were connected by electrical wires to their power supplies located outside the climatic chamber, which replaced the alkaline batteries normally used during atmospheric radiosoundings. This enabled the acquisition of measurements, with the radiosondes both outside and inside the climatic chambers, for many hours without interruptions for replacing the batteries. Figure 3 shows the measurement layout inside the Kambic chamber. At a distance of 3 cm from the temperature sensor of each radiosonde, a Pt100 reference thermometer traceable to SI standards was placed and fixed to the plastic grid. Moreover, an additional Pt100 reference thermometer was placed in the middle of the measurement frame, at the same distance of about 7.5 cm from the two radiosondes' temperature sensors. The reference thermometers were also connected to their own reading unit located outside the chambers. Figure 4 shows a schematic of the measurement layout, where the reference thermometers and their position with respect to radiosondes' sensors are also represented.

The intercomparison was carried out in two separate stages described in the Sect. 3.1 and Sect. 3.2.

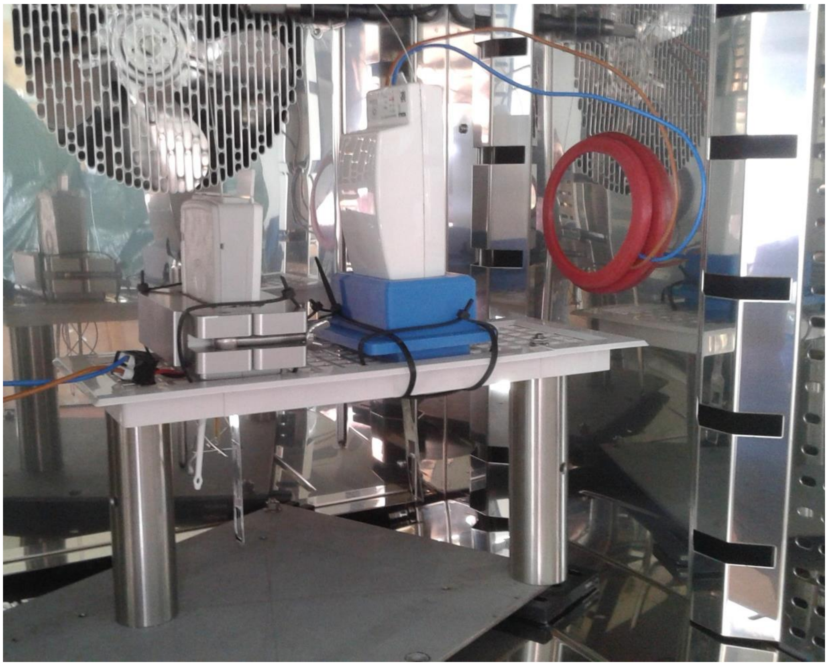

Figure 3: Photo of the measurement layout inside the Kambic chamber, with the frame including the plastic grid, the metal plate at the basis, the cylindrical steel holders, the radiosondes RS92 (left) and RS41 (right) with their sensor booms vertically oriented each in opposition to the other. The two radiosondes, supported by two adapters fixed to the grid with plastic ties passing through the holes of the grid, were connected by electrical wires to their power supplies located outside the chamber.

https://doi.org/10.5194/amt-2021-337
Preprint. Discussion started: 21 October 2021

Atmospheric Measurement Techniques Discussions

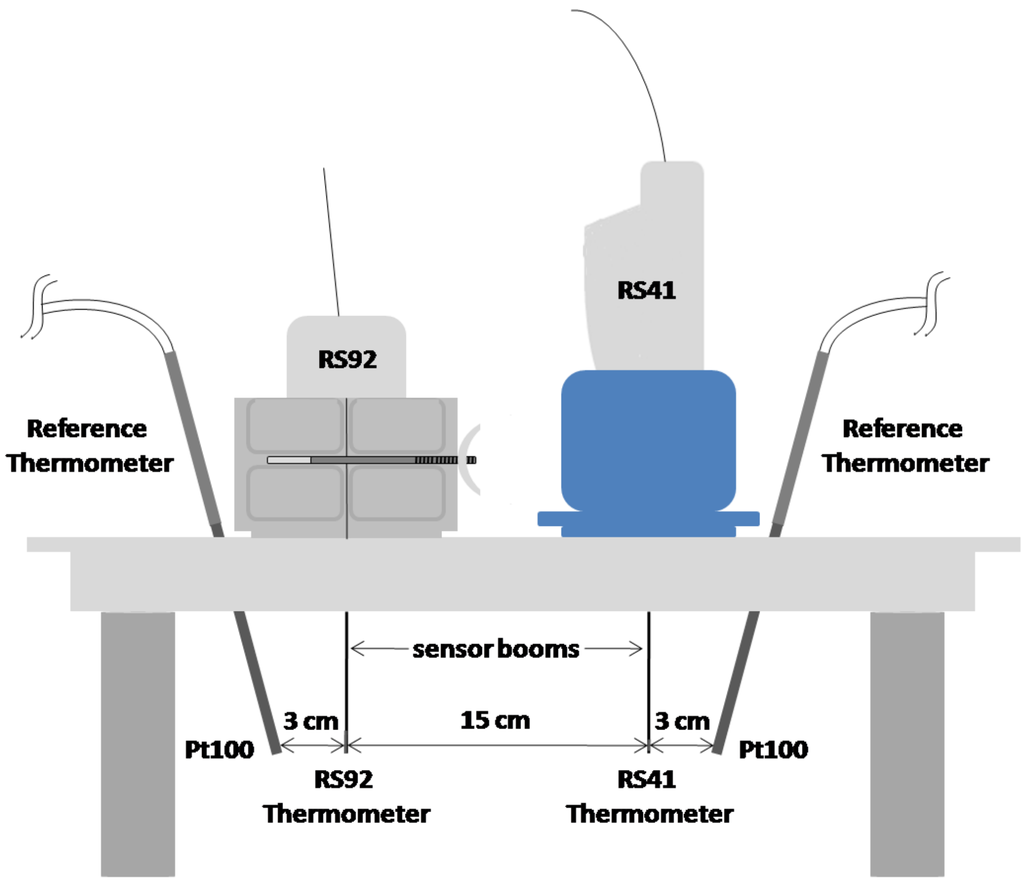

Figure 4: Scheme of the measurement layout: the sensor booms of the two radiosondes and their thermometers were located at 15 cm distance, while a Pt100 reference thermometer was at 3 cm from the temperature sensor of each radiosonde. An additional Pt100 reference thermometer (not shown) was placed in the middle, at a distance of about 7.5 cm from each radiosonde's temperature sensor.

3.1 Tests using a single climatic chamber

At the first stage, a pair of RS41 and RS92 radiosondes has been tested inside the Kambic chamber at different temperature and humidity conditions, at ambient pressure. A fan placed on the back inner wall of the chamber blows the air in, which, after passing through the chamber internal components, is conveyed inside the chamber measurement volume, where it is distributed uniformly both laterally and from below. In this way, the temperature and humidity are kept homogeneous inside the chamber.

Simultaneous measurements from the radiosondes and the reference thermometers were acquired at nine conditions of temperature (T) and relative humidity (RH), as reported in Table 1. The chamber cannot dynamically control the relative humidity at $T \leq 0$ °C, while for positive temperatures three different RH values have been set, corresponding to low (RH = 20 %), moderate (RH = 60 %) and very high (RH = 98/95 %) humidity conditions. The above conditions of T and RH have been selected to reproduce the atmospheric conditions that radiosondes meet at the ground, at different climatic regions and seasons.

For each *T* and *RH* condition, measurements from all the sensors in the chamber have been acquired only after thermal stability was achieved, which required a time period up to several hours. The thermal stability within the chamber was considered achieved when the minimum temporal variability was observed in readings of all reference thermometers. The temporal resolution of measurements was 1 s for radiosondes and 3 s for reference thermometers, while the duration of the acquisition loop ranged from 5-10 min, corresponding to at least 300 repeated measurements for each radiosonde sensor.

Before placing the radiosondes in the climatic chamber, the pre-launch ground check procedure recommended by the manufacturer was performed, using GC25 and RI41 devices for RS92 and RS41, respectively. In this way, the radiosondes have been tested inside the chamber simulating the complete pre-launch phase in radiosoundings. Moreover, the raw data of radiosonde temperature measurements have been used, without the corrections applied by the Vaisala or GRUAN data processing algorithms (i.e., the correction for warm/cold bias due to solar/infrared radiation in daytime/nighttime launches, the time lag correction and the ground check correction for RS92 measurements only).

As an example, Fig. 5 shows the plots of temperature measurements from both the radiosondes and the reference thermometers acquired at T = 20 °C and RH = 20 % for a period of 8 min, corresponding to 480 repeated measurements for radiosondes' temperature sensors.

Kambic settings	Temperature (°C)	Relative humidity (%)
1	-40	Off
2	-20	Off
3	0	Off
4	20	20
5	20	60
6	20	98
7	40	20
8	40	60
9	40	95

Table 1: Temperature and relative humidity values corresponding to the nine different measurement conditions reproduced in the Kambic chamber (Kambic settings). At negative temperatures and 0 °C, the relative humidity in the chamber cannot be dynamically controlled.

https://doi.org/10.5194/amt-2021-337
Preprint. Discussion started: 21 October 2021

Atmospheric Measurement Techniques Discussions

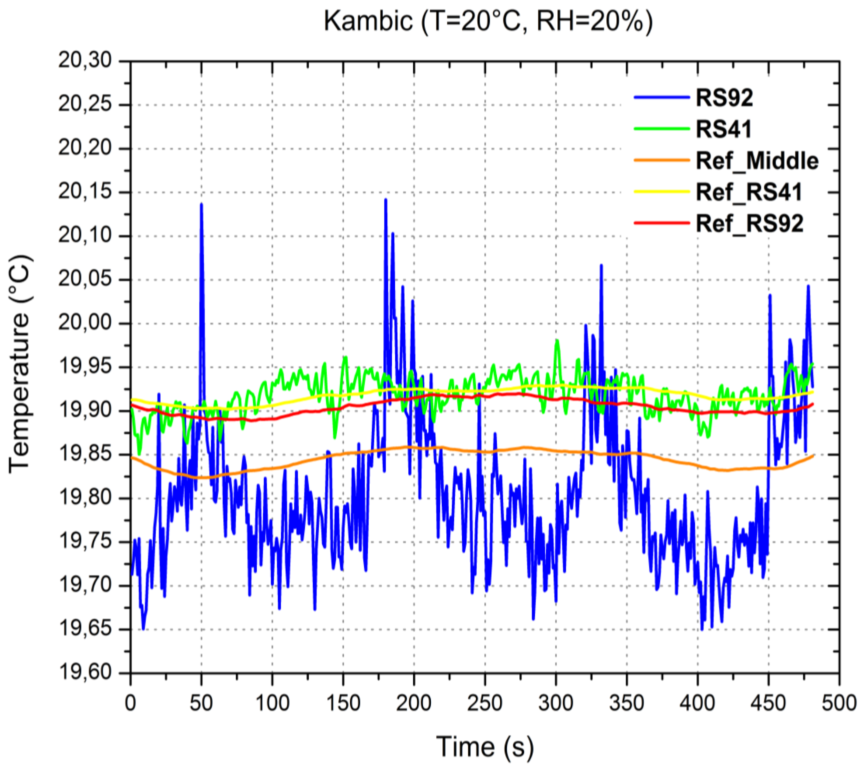

Figure 5: Time series of temperature measurements (vertical axis) from all the sensors in the Kambic chamber set at T = 20 °C and RH = 20 %. The duration of the acquisition was 480 s (8 min), corresponding to 480 repeated measurements for radiosondes' sensors. The blue line refers to the RS92, the green to the RS41, the red and yellow to the reference thermometer close to the temperature sensor of RS92 and RS41, respectively, the orange to the reference thermometer in the middle of the measurement frame (i.e., between radiosondes' temperature sensors).

In order to compare RS41 and RS92 and characterize their differences, the mean and standard deviation of measurements from all the temperature sensors in the chamber, as well as of other measurement derived quantities (detailed below in this section), have been calculated over the whole acquisition period for each condition of T and RH set in the chamber. The standard deviation of readings from each temperature sensor results from the combination of sensor's noise and chamber instability. The latter was measured as the standard deviation of reference thermometers' readings in the points where these thermometers were placed, assuming their noise negligible. This measure of the chamber instability made it possible to estimate the noise of radiosondes' temperature sensors.

The chamber temperature inhomogeneity (or uniformity) through the measurement volume was measured as the maximum difference between the mean values of reference thermometers' measurements.

From the results of the laboratory tests (Sect. 4.1.2), it was found that the chamber inhomogeneity through the portion of the measurement volume between the temperature sensor of each radiosonde and the co-located Pt100 reference thermometer is typically less than 0.05 °C and does not affect the temperature difference between these sensors, $\Delta T(sonde, ref\_therm)$. The latter can be considered as an estimate of the sonde calibration error, $Err_{cal}(sonde)$, that is:

$$\Delta T(sonde, ref\_therm) = Err_{cal}(sonde) \quad (1)$$

The calibration errors of radiosondes' temperature sensors have been evaluated by calculating the mean of $\Delta T(sonde, ref\_therm)$ over the acquisition period for each *T* and *RH* condition and can be expressed as:

$$\Delta T_{mean}(sonde, ref\_therm) = Err_{cal}^{mean}(sonde) \qquad (2)$$

The repeatability in calibration errors of radiosondes' temperature sensors has been calculated as the standard deviation of $\Delta T(sonde, ref\_therm)$.

The temperature difference (i.e., bias) between RS41 and RS92, $\Delta T(RS41, RS92) = T_{RS41} - T_{RS92}$, can be affected by the chamber inhomogeneity through the measurement volume and it may not represent the real temperature difference between the two sondes. Therefore, instead of this difference, it was considered the temperature absolute difference between the two sondes, $\Delta T_{abs}(RS41, RS92)$, defined, at any instant, as the difference between their calibration errors:

$$\begin{aligned}\Delta T_{abs}(RS41, RS92) &= \Delta Err_{cal}(RS41, RS92) = Err_{cal}(RS41) - Err_{cal}(RS92)\\ &= \Delta T(RS41, ref_{RS41}) - \Delta T(RS92, ref_{RS92}) \qquad (3)\end{aligned}$$

$\Delta T_{abs}(RS41, RS92)$ is not affected by the chamber inhomogeneity, being the inhomogeneity between the thermometer of each radiosonde and the co-located reference thermometer negligible.

The temperature bias between RS41 and RS92 has been evaluated by calculating the mean of $\Delta T_{abs}(RS41, RS92)$, that is:

$$\Delta T_{abs}^{mean}(RS41, RS92) = \Delta Err_{cal}^{mean}(RS41, RS92) \qquad (4)$$

The repeatability in the temperature bias has been calculated as the standard deviation of $\Delta T_{abs}(RS41, RS92)$.

3.2 Fast temperature changes using two climatic chambers

At the second stage of the experiment, the same pair of radiosondes tested during the first stage was tested before and after a series of fast temperature changes, generated by quickly moving (within ≈ 10 s) the measurement frame from the Kambic chamber to the adjacent Weiss Technik chamber and vice versa, with the two chambers set at different temperatures. Each chamber was also equipped with a Pt100 reference thermometer fixed to an inner wall. Both rising and dropping temperature changes of about 20 °C were performed, and more specifically two rising changes from 0 °C to 20 °C and two dropping changes from 20 °C to 0 °C and -5 °C. The Kambic was set at 0 °C and -5 °C, the Weiss Technik at 20 °C. The objective was to study the effects of such changes on the temperature sensors of both radiosondes. A step of about 20 °C was selected to simulate a steep thermal change that a radiosonde may meet when passing from the indoor of a laboratory or inflation chamber to outdoor conditions before launch.

Simultaneous measurements from radiosondes' temperature sensors and reference thermometers have been acquired before and after each change as in the first stage, after thermal stability was achieved in the respective chamber, with same temporal resolutions and similar acquisition durations. A period of about 2 h, longer than the typical duration of a radiosounding, preceded the acquisition before each change. However, in order to study the potential effects of the temperature changes on the measurements of radiosoundings, i.e. within their duration, the acquisition period

https://doi.org/10.5194/amt-2021-337
Preprint. Discussion started: 21 October 2021

Atmospheric Measurement Techniques Discussions
Open Access
EGU

considered after each change was started as soon as the thermal stability was reached in the chamber, typically about 15 min after the change. As at the first stage, the manufacturer ground check procedures were performed before the chamber tests, in order to test the radiosondes under conditions similar to those before launch in radiosoundings, and only raw measurements from radiosondes were acquired.

As an example, Fig. 6 shows the plots of temperature measurements from both the radiosondes and the reference thermometers acquired before and after a quick change from 0 °C to 20 °C for a period of about 27 min.

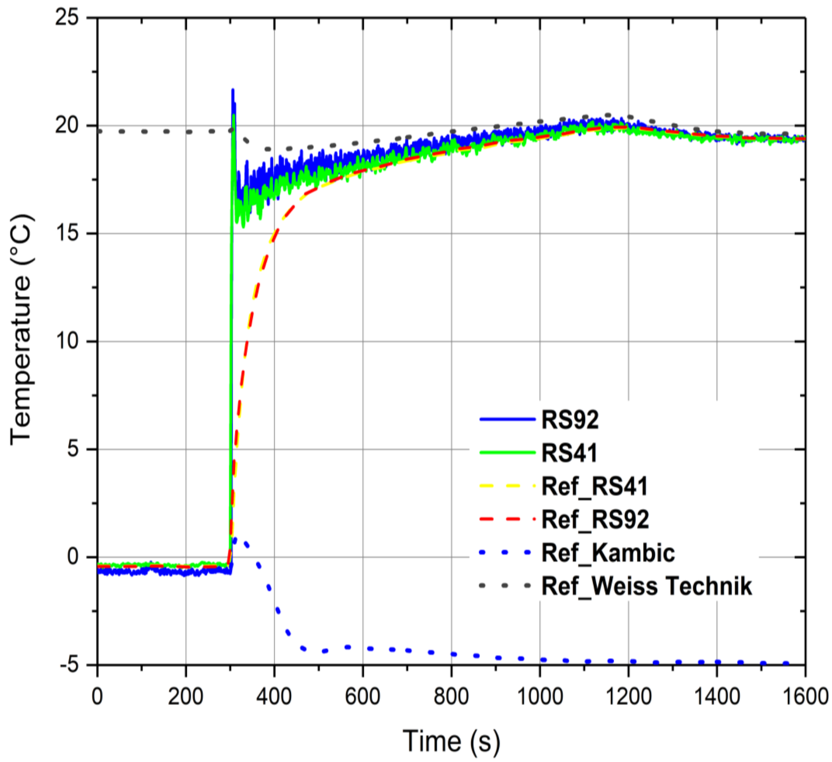

Figure 6: Time series of temperature measurements (vertical axis) from both the radiosondes and the reference thermometers acquired before and after a change from 0 °C to 20 °C for a period of 1600 s (about 27 min). Solid lines refer to the radiosondes (blue for RS92, green for RS41), dashed lines refer to the reference thermometers close to radiosondes' sensors (red for RS92 and yellow for RS41), dotted lines refer to the reference thermometers fixed to chambers' inner walls (blue for the Kambic chamber set at 0 °C before the change and gray for the Weiss Technik chamber set at 20 °C).

The effects of the fast temperature changes on the temperature sensors of both radiosondes have been studied and compared by considering the same quantities described in Sect. 3.1, that is, in terms of sensors' noise, as well as of their calibration error and bias with related repeatability. These quantities were calculated over the acquisition period under thermal stability conditions in the chambers, both before and after each change. For example, for the change shown in Fig. 6 the acquisition period under stability conditions in the first chamber (set at 0°C) before the change was 5 min (from 0-300 s in Fig. 6), while the corresponding acquisition period in the second chamber (set at 20°C) after the change was the last 5 min of acquisition (from 1300-1600 s in Fig. 6), starting about 17 min after the change.

Atmospheric Measurement Techniques Discussions

4 Results

4.1 Tests in the Kambic chamber

In this section, the results obtained during the first stage of the experiment, described in Sect. 3.1, are reported and discussed. More specifically, Sect. 4.1.1 concerns the noise characterization of RS92 and RS41 temperature sensors, Sect. 4.1.2 refers to RS92 and RS41 calibration errors with their uncertainties, section 4.1.3 refers to the temperature bias between RS92 and RS41 and the related uncertainty.

4.1.1 Noise of RS92 and RS41 temperature sensors

The standard deviations of temperature measurements from all the sensors in the chamber for all *T* and *RH* conditions considered (see Table 1) are plotted in Fig. 7. The standard deviations from reference thermometers (red, yellow and orange stars for the thermometer close to RS92, to RS41 and in the middle of measurement frame, respectively) represent an estimate of the chamber instability in the points where these thermometers were placed. For each *T* and *RH* condition, the chamber instability is uniform through the measurement volume, being the standard deviations from all reference thermometers very similar, and significantly lower than the standard deviation from both radiosondes' temperature sensors (blue and green circles for RS92 and RS41, respectively). More specifically, for each condition of *T* and *RH* the chamber instability is lower than 0.014 °C, with uniformity of instability (measured as maximum difference between the chamber instabilities) within ±0.006 °C, except for *T* = -20 °C, where the instability is slightly higher, while remaining less than 0.03 °C, and less uniform (within ±0.012 °C). These values of the chamber instability are significantly lower than those reported in the manufacturer specifications, typically lower than 0.1 °C.

The high chamber stability compared to the standard deviations from radiosondes' temperature sensors, together with the high uniformity in the chamber instability, allowed to characterize the noise of these sensors and related differences. Indeed, the standard deviations from radiosondes' sensors, resulting from the combination of sensors' noise and chamber instability, represent an estimate of that noise. Moreover, the difference or the ratio between the noise estimates for the two radiosondes' sensors is not affected by a different chamber instability in the points where these sensors were placed. The plots shown in Fig. 7 reveal that for each *T* and *RH* condition, the noise of RS41 temperature sensor (green circles) is lower than that of RS92 (blue circles). More specifically, the noise for RS41 ranges from 0.016 °C (*T* = 40 °C, *RH* = 95 %) to 0.064 °C (*T* = -20 °C), while the noise for RS92 ranges from 0.073 °C (*T* = -40 °C) to 0.1 °C (*T* = -20 °C). In terms of noise ratio, the RS92 temperature sensor is from 1.6 (*T* = -20 °C) to 5.3 (*T* = 40 °C, *RH* = 20 %) times noisier than that of RS41.

At *T* = -20 °C, where the noise is maximum for both the radiosondes (≈ 0.06 °C for RS41 and ≈ 0.1 °C for RS92) the chamber instability is also maximum (ranging from 0.015 °C to 0.027 °C). In this case, a higher chamber instability leads to overestimating the noise of both radiosondes' sensors, being this noise estimated as the standard deviation of sensors' measurements, which is more contaminated by the chamber instability.

https://doi.org/10.5194/amt-2021-337
Preprint. Discussion started: 21 October 2021

Atmospheric Measurement Techniques
Discussions

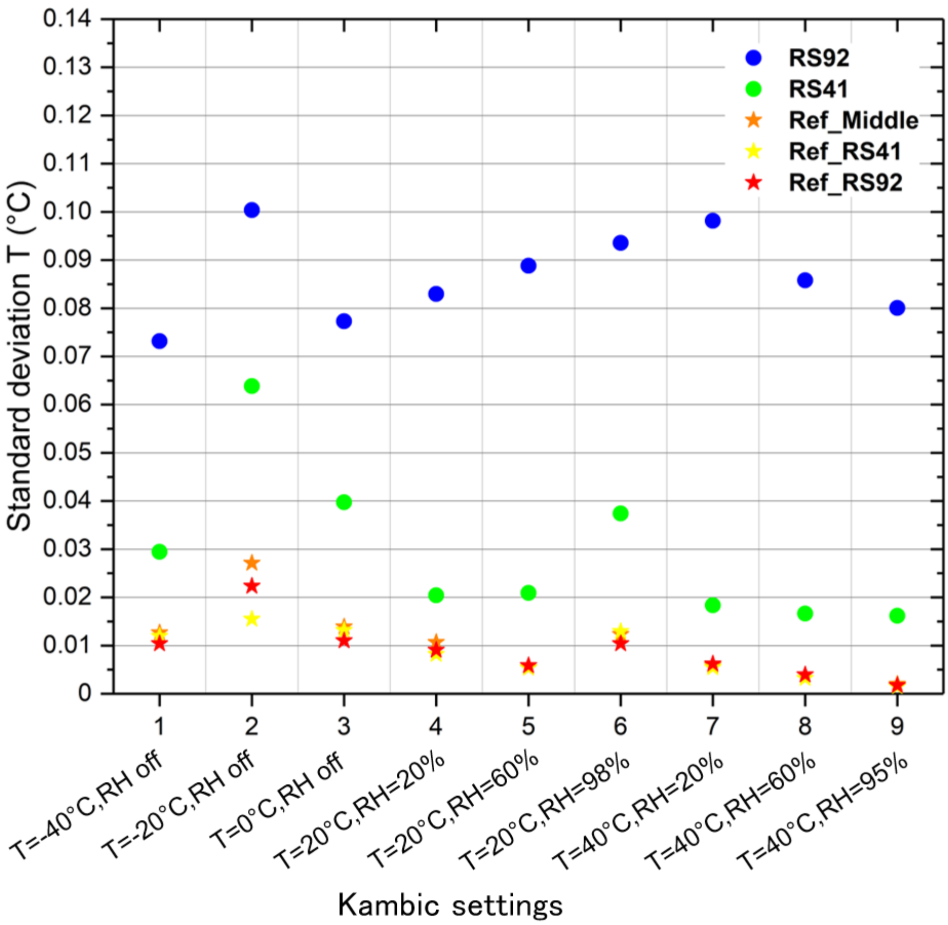

Figure 7: Standard deviations of temperature measurements (vertical axis) from the radiosondes (circles) and the reference thermometers (stars) calculated at the different temperature (*T*) and relative humidity (*RH*) conditions in the Kambic chamber (horizontal axis). At $T \leq 0$ °C there is no relative humidity control in the chamber (*RH* off). The blue and green circles refer to RS92 and RS41, respectively. The red, yellow and orange stars refer to the reference thermometer close to RS92, to RS41 and in the middle of measurement frame, respectively.

4.1.2 RS92 and RS41 calibration errors and uncertainties

In Fig. 8 the mean and the standard deviation of $\Delta T(sonde, ref\_therm)$ calculated for each T and RH condition set in the chamber are plotted (blue and green plot for RS92 and RS41, respectively). The chamber inhomogeneity through the measurement volume, measured as the maximum difference between the mean values of reference thermometers' readings, is also reported for all the measurement conditions (red vertical bars). The values of this inhomogeneity are within ±0.15 °C, with a minimum of ±0.07 °C (T = 0 °C; T = 20 °C, RH= 20 %), except for T = -40 °C where the inhomogeneity is within ±0.29 °C. These values are significantly lower than those reported in the manufacturer specifications, typically within ±0.3 °C. It is reasonable to assume that the chamber inhomogeneity between each radiosonde's temperature sensor and the co-located reference thermometer is significantly lower than the above values and does not appreciably affect the values of $\Delta T(sonde, ref\_therm)$. Indeed, assuming the chamber inhomogeneity linearly dependent on the distance and considering the distances between the reference thermometers and between each radiosonde's temperature sensor and the co-located reference thermometer, the inhomogeneity between these latter sensors can be estimated from 3 to 7 times lower than the above values and typically less than 0.05 °C. Thus, Eqs. (1) and (2) can be considered valid and the means and standard deviations of $\Delta T(sonde, ref\_therm)$ shown in Fig. 8 represent, respectively, the calibration errors and related repeatabilities of radiosondes' temperature sensors.

The plots in Fig. 8 show that, for each *T* and *RH* condition set in the chamber, the calibration error and related repeatability of RS41 temperature sensor are smaller than those of RS92, indicating that RS41 is more accurate than RS92. The lower repeatability in the calibration error for RS41 is due to the lower noise level of its temperature sensor compared to RS92, as shown in the previous section.

More specifically, the calibration error of RS41 temperature sensor, $\mathrm{Err}_{cal}^{mean}(RS41) = \Delta T_{mean}(RS41,\ ref\_RS41)$, assumes both negative and positive values, ranging from -0.05 °C (*T* = -20 °C) to 0.08 °C (*T* = 40 °C, RH = 95 %), indicating the absence of systematic bias in the calibration and a correction factor less than 0.1 °C for all considered *T* and *RH* conditions. The repeatability in the calibration error of this sensor is lower than 0.04 °C at all conditions, except for *T* = -20 °C, where it reaches the maximum value of 0.06 °C, which represents an overestimation due to a higher chamber instability observed at this temperature. The total calibration uncertainty results from the combination of repeatability (A-type uncertainty) and further B-type uncertainty contributions. The latter comprise the calibration uncertainty of the reference thermometer (0.01 °C for *T* < 0 and 0.005° for *T* > 0), the uncertainty of sensors' reading systems (0.01 °C for both the radiosonde's sensor and the reference thermometer) and the uncertainty due to the chamber inhomogeneity between the radiosonde's sensor and the reference thermometer. The B-type uncertainty contributions are small compared to repeatability and do not significantly contribute to the total calibration uncertainty.

The above values of RS41 calibration error and related uncertainty are in very good agreement with those measured in laboratory tests performed by the manufacturer, who reports a calibration error ranging from -0.08 °C to 0.06 °C, resulting from tests with 5 different RS41 units at various temperatures from -98 °C to 39 °C (Vaisala, 2017a), and a calibration repeatability (*k* = 2) less than 0.1 °C (Survo et al., 2014; Vaisala, 2017a). Moreover, there is also consistency with GRUAN laboratory tests, carried out with more than 150 RS41 units at room temperature under various humidity conditions inside multiple standard humidity chambers equipped with Pt100 reference thermometers (Dirksen et al., 2020). The GRUAN tests indicate a cold bias in the calibration of 0.025 °C and a calibration uncertainty (*k* = 1) less than 0.2 °C.

For RS92 temperature sensor, the calibration error estimated in our experiment, $\mathrm{Err}_{cal}^{mean}(RS92) = \Delta T_{mean}(RS92,$ $ref_$RS92), is negative under all *T* and *RH* conditions set in the chamber, ranging from -0.31 °C (*T* = 40 °C, *RH* = 20 %) to -0.08 °C (*T* = 40 °C, *RH*= 95 %), indicating a cold bias in the calibration, with a correction factor ranging from at least 0.1 °C up to a few tenths of a degree. The repeatability in the calibration error is less than 0.1 °C under all considered conditions. The total calibration uncertainty results from the combination of the repeatability and the same B-type uncertainty contributions described above, which are negligible compared to repeatability as for RS41. The values of calibration uncertainty estimated for RS92 temperature sensor are 0.025 °C higher than those provided by the manufacturer, who reports a calibration repeatability (*k* = 2) of 0.15 °C (Vaisala, 2013; Jauhiainen et al., 2014). On the other hand, this uncertainty contribution has never been characterized with manufacturer-independent laboratory tests, and in the GRUAN data processing it is evaluated by combining the value provided by the manufacturer with the temperature correction factor ΔT_{RS92}^{GC25}, resulting from the pre-launch ground check performed with the GC25 (Dirksen et al., 2014).

Atmospheric Measurement Techniques Discussions

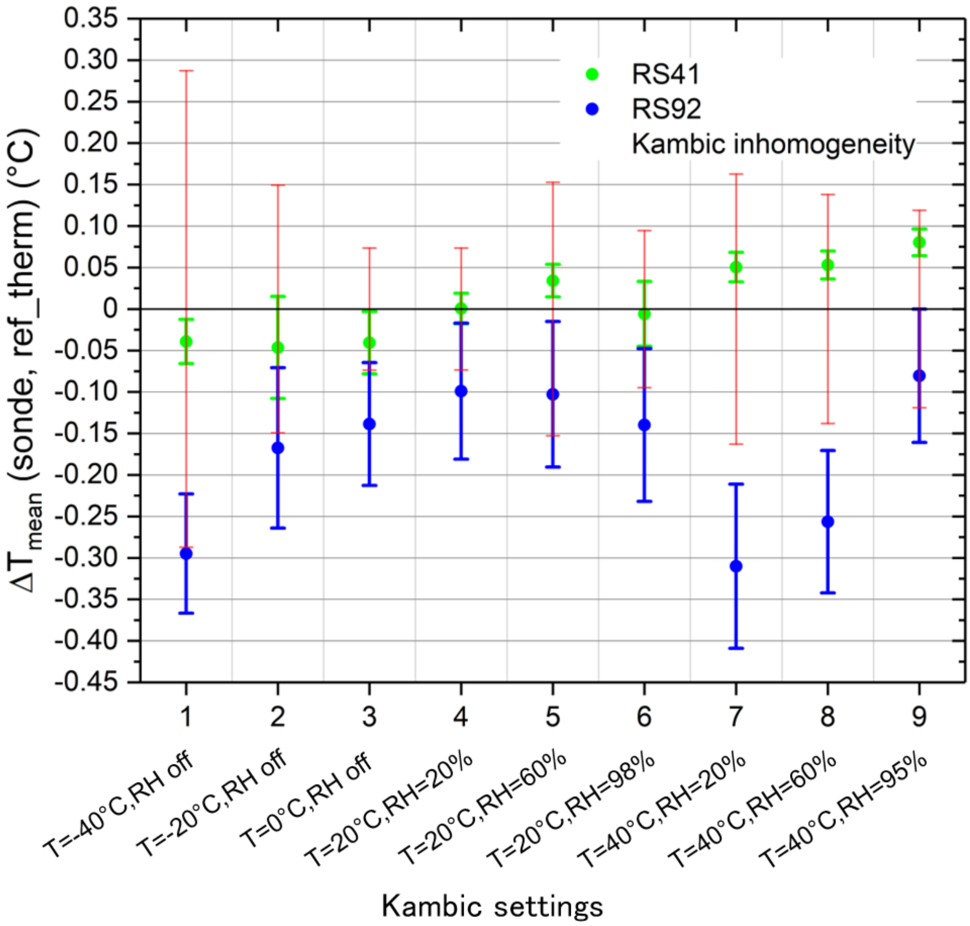

Figure 8: Mean (circles) and standard deviation (vertical bars) of the temperature difference between each sonde and its co-located reference thermometer (vertical axis), for all the temperature (*T*) and relative humidity (*RH*) conditions set in the Kambic chamber (horizontal axis). The green plot refers to the RS41, the blue plot to the RS92. Red vertical bars represent the chamber inhomogeneity through the measurement volume.

Finally, Table 2 provides the values of ΔT_{RS92}^{GC25} determined before testing the radiosondes inside the climatic chamber. The same values of ΔT_{RS92}^{GC25} for different *T* and *RH* conditions refer to a single ground check procedure performed before testing the radiosondes under those conditions during a single measurement session without interruptions. ΔT_{RS92}^{GC25} is always negative, ranging from -0.27 °C to – 0.15 °C, indicating a warm bias of RS92 temperature sensor compared to the Pt100 thermometer inside the GC25 chamber. Therefore, the application of this correction to RS92 temperature sensor leads to an increase of the difference between this sensor and the co-located reference thermometer, that is the calibration error (blue circles in Fig. 8), making its measurement accuracy worse. This is due to possible long-term instability or drifts in the calibration of the Pt100 thermometer inside the GC25 chamber, which requires further investigation.

https://doi.org/10.5194/amt-2021-337
Preprint. Discussion started: 21 October 2021

Atmospheric Measurement Techniques Discussions

Kambic settings	ΔT_{RS92}^{GC25} (°C)
1	-0.18
2	-0.18
3	-0.15
4	-0.15
5	-0.15
6	-0.15
7	-0.27
8	-0.27
9	-0.27

Table 2: Values of the correction factor ΔT_{RS92}^{GC25} for RS92 temperature sensor resulting from the GC25 and determined before testing the radiosondes inside the Kambic chamber under different temperature and humidity conditions (Kambic settings).

The above results confirm independently of the manufacturer that the calibration error and uncertainty of RS41 temperature sensor meet the highest quality standards of reference Platinum resistor thermometers and, therefore, this sensor type does not need of a pre-launch ground check correction to be applied to radiosounding temperature measurements. However, RS92 temperature sensor requires both such a correction with the GC25 and periodic high quality assurance checks of the calibration of the Pt100 reference thermometer inside the GC25 chamber, to avoid cold biases in radiosounding temperature measurements in the order of a few tenths of a degree or higher. Indeed, a not reliable ground check correction with the GC25 can make the measurement accuracy worse rather than improving it, as occurred in our experiment. In any case, the calibration uncertainty of RS92 temperature sensor is higher than that of RS41.

4.1.3 RS41 and RS92 temperature bias and uncertainty

Figure 9 shows the mean temperature absolute bias between RS41 and RS92, $\Delta T_{abs}^{mean}(RS41, RS92)$, as defined in Eq. (4), and the related repeatability (vertical bars) calculated for all *T* and *RH* conditions set in the chamber. $\Delta T_{abs}^{mean}(RS41, RS92)$ is positive under all conditions, ranging from 0.1 °C (*T* = 0 °C; *T* = 20 °C, *RH* = 20 %) to 0.36 °C (*T* = 40 °C, *RH* = 20 %), which indicates that RS92 is colder than RS41, mainly due to the cold bias in the calibration of RS92 temperature sensor discussed in Sect. 4.1.2. The repeatability in $\Delta T_{abs}(RS41, RS92)$, as defined in Sect. 3.1, is less than 0.1 °C under all considered conditions and it represents the total uncertainty in the temperature absolute bias, being all B-type uncertainty contributions negligible.

https://doi.org/10.5194/amt-2021-337
Preprint. Discussion started: 21 October 2021

Atmospheric Measurement Techniques
Discussions

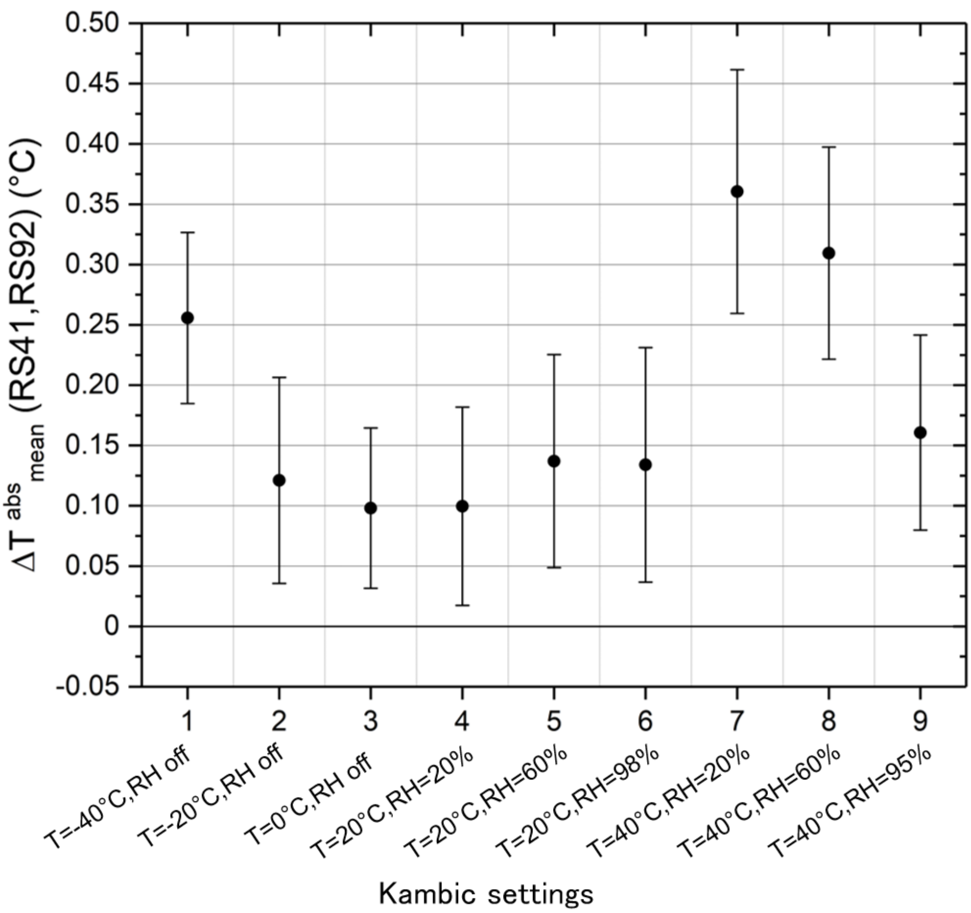

Figure 9: Mean temperature absolute difference between RS41 and RS92, $\Delta T_{abs}^{mean}(RS41, RS92)$ (vertical axis), for all the temperature (*T*) and relative humidity (*RH*) conditions set in the Kambic chamber (horizontal axis); the vertical bars represent the repeatability in $\Delta T_{abs}(RS41, RS92)$, calculated as the standard deviation.

The above results for the temperature bias between RS41 and RS92 are not directly comparable with those resulting from dual soundings, carried out both by the manufacturer and within GRUAN, due to the different calculation methods and measurements conditions. In dual soundings, the average and standard deviation of the measurement differences from multiple pairs of RS41 and RS92 radiosondes are calculated at each altitude level, assuming the two radiosondes exposed to the same atmospheric conditions during each sounding. Moreover, the measurement profiles are smoothed (with a vertical resolution typically ranging from 10 m up to 2 km) and the measurement data used to calculate the differences are processed with Vaisala or GRUAN algorithms, where the corrections mentioned in Sect. 3.1 are applied to raw measurements. In our laboratory tests inside the Kambic chamber, the mean and the standard deviation of the difference between the calibration errors of the considered pair of RS41 and RS92, $\Delta T_{abs}(RS41, RS92)$, have been calculated using repeated radiosondes' raw measurements over time, to which no correction was applied.

On the other hand, in dual soundings the measurements are performed at decreasing pressure levels and with the sensors exposed to solar radiation, for daytime soundings only, and the ventilation resulting from the combination of the balloon lifting vertical speed (typically 5 m/s), the horizontal wind and radiosonde's pendulum motions and rotations. Differently, in the Kambic the measurements are performed at laboratory ambient pressure and with the weak ventilation on the sensors generated by the chamber.

Despite the above differences between dual soundings and our tests in the climatic chamber in order to determine the temperature bias between RS41 and RS92, we can compare to some extent the results of our experiment with those resulting from nighttime dual soundings at the ground. In such conditions, the corrections of temperature measurements due to the time lag and infrared radiation implemented in Vaisala and GRUAN data processing are negligible (Vaisala, 2010; Dirksen et al. 2014; Vaisala, 2017a). Thus, the difference between the raw measurements in the climatic chamber and the measurements used in dual soundings is essentially due to the ground check correction applied to RS92 measurements in dual soundings only. Therefore, recalculating $\Delta T_{abs}(RS41, RS92)$ by applying to RS92 measurements the ground check correction ΔT_{RS92}^{GC25}, a temperature bias comparable to that of nighttime dual soundings at the ground should in principle be obtained. However, the values of ΔT_{RS92}^{GC25} reported in Table 2 are not reliable and worsen the measurement accuracy of RS92 temperature sensor rather than improve it, as shown in the previous section. As a consequence, the correction corresponding to the mean calibration error of RS92 temperature sensor, $\mathrm{Err}_{cal}^{mean}(RS92)$ (blue circles in Fig. 8), was applied instead of ΔT_{RS92}^{GC25}. Such a correction is appropriate instead of ΔT_{RS92}^{GC25}, as it comes from the comparison of RS92 temperature sensor with the co-located Pt100 reference thermometer. Applying this correction, by replacing T_{RS92} with $T_{RS92} - \mathrm{Err}_{cal}^{mean}(RS92)$, the corrected temperature absolute bias, comparable to that in nighttime dual soundings at the ground, was obtained:

$$\Delta T'_{abs}(RS41, RS92) = \Delta T_{abs}(RS41, RS92) + \mathrm{Err}_{cal}^{mean}(RS92) \tag{5}$$

Figure 10 shows the mean $\Delta T'^{mean}_{abs}(RS41, RS92)$ and the standard deviation or repeatability (vertical bars) of the corrected temperature bias, as defined in Eq. (5), for each measurement condition set in the chamber. The standard deviation represents the uncertainty in the corrected temperature bias. The results reveal that $\Delta T'^{mean}_{abs}(RS41, RS92)$ ranges from -0.05 °C (T = -20 °C) to 0.08 °C (T = 40 °C, RH = 95 %), indicating that RS41 can be colder or warmer than RS92, with a temperature bias less than 0.1 °C in absolute value. The uncertainty in the temperature bias is lower than 0.1 °C.

These findings are similar to the means and standard deviations of temperature differences between RS41 and RS92, typically within ± 0.1 °C and 0.2 °C respectively, calculated in nighttime dual soundings performed at different latitudes both by the manufacturer (Jauhiainen et al., 2014; Vaisala, 2014) and independently within GRUAN (Jensen et al., 2016; Kawai et al., 2017; Dirksen et al., 2020; Jing et al., 2021), not only at near surface, but throughout the troposphere. Moreover, the values of the temperature bias and the related uncertainty obtained from the laboratory tests in the climatic chamber in principle refer to the radiosondes at the ground before launch, while the corresponding values resulting from dual soundings never refer to the radiosondes at the ground, but at higher altitudes after launch. Thus, the results from the tests in the climatic chamber represent an additional information to that provided by dual soundings for the characterization of the temperature bias between RS41 and RS92.

https://doi.org/10.5194/amt-2021-337
Preprint. Discussion started: 21 October 2021

Atmospheric Measurement Techniques Discussions

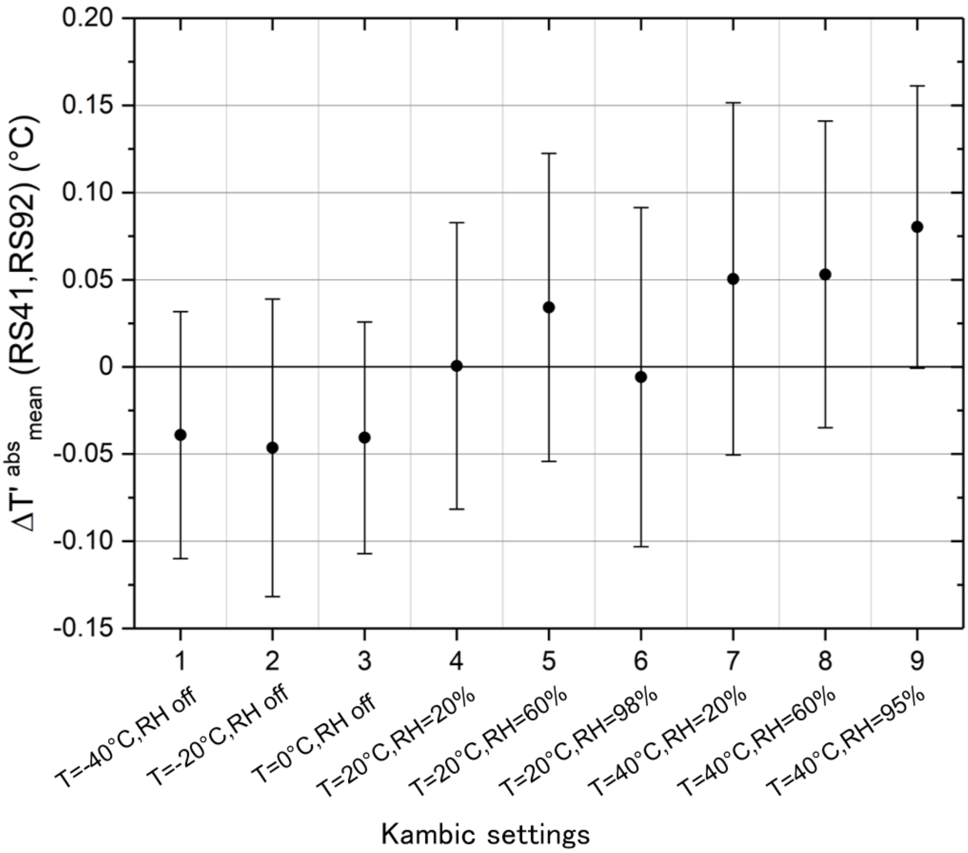

Figure 10: Mean corrected temperature bias between RS41 and RS92, $\Delta T'^{mean}_{abs}(RS41, RS92)$ (vertical axis), for all the temperature (*T*) and relative humidity (*RH*) conditions set in the Kambic chamber (horizontal axis); the vertical bars represent the repeatability in $\Delta T'_{abs}(RS41, RS92)$, calculated as the standard deviation.

4.2 Fast temperature changes

In this section, the outcome of the second stage of the experiment, described in Sect. 3.2, is discussed. The effects of fast temperature changes on RS92 and RS41 temperature sensors have been investigated in terms of noise (Sect. 4.2.1), calibration error and its uncertainty (Sect. 4.2.2), bias and related uncertainty (Sect. 4.2.3).

4.2.1 Noise of RS92 and RS41 temperature sensors

Table 3 reports the values of chamber instability and noise of RS41 and RS92 temperature sensors before and after the fast temperature changes described in Sect. 3.2 (i.e.: two rising changes from 0 °C to 20 °C and two dropping changes from 20 °C to 0 °C and -5 °C). The temporal sequence of changes is also reported. As in Sect. 4.1.1, the chamber instability and the noise of radiosondes' sensors are measured as the standard deviation of readings from reference thermometers and radiosondes' sensors, respectively.

https://doi.org/10.5194/amt-2021-337
Preprint. Discussion started: 21 October 2021

Atmospheric Measurement Techniques Discussions

T Rise (°C)	Before change			After change		
	Chamber instability	RS41 noise	RS92 noise	Chamber instability	RS41 noise	RS92 noise
"0+20" #1	0.02	0.04	0.12	0.01	0.09	0.13
"0+20" #3	0.02	0.05	0.10	0.01	0.13	0.17
T Drop (°C)	Before change			After change		
	Chamber instability	RS41 noise	RS92 noise	Chamber instability	RS41 noise	RS92 noise
"20-5" #4	0.02	0.05	0.09	0.02	0.13	0.27
"+20-0" #2	0.01	0.03	0.04	0.01	0.10	0.28

Table 3: Chamber instability and noise of RS41 and RS92 temperature sensors before and after the two rising changes from 0 °C to 20 °C (yellow rows) and the two dropping changes from 20 °C to 0 °C and -5 °C (gray rows). The numbers next to each temperature change in the left column indicate the time sequence of changes.

The results reported in Table 3 show that before each temperature change, the noise of both RS41 and RS92 temperature sensors is the same as in the first stage of the experiment, with values lower than 0.05 °C and 0.1 °C for RS41 and RS92, respectively. After each change, an increase in the noise of both radiosondes' temperature sensors is observed and this increase is maximum for the RS92 and dropping changes. The values of noise after changes are typically of 0.1 °C for RS41 and from 0.1 °C to 0.3 °C for RS92. However, the noise increase after each change is a transient effect observed as soon as the thermal stability was reached in the chamber (typically about 15 min after the change), fading within the following 2 h, as it is evident from the noise values observed before the next change. Such an effect may affect the measurements of radiosoundings where radiosondes meet a fast and steep thermal change when passing from the indoor of a laboratory or inflation chamber, where the ground check procedures are usually performed, to outdoor condition before launch.

4.2.2 RS92 and RS41 calibration errors and uncertainties

Table 4 reports the values of calibration error Err_{cal} and related uncertainty $U(Err_{cal})$ of both RS41 and RS92 temperature sensors before and after the temperature changes described in section 3.2. For each radiosonde the calibration error is evaluated as in Sect. 4.1.2, while the calibration uncertainty results from the combination in quadrature of the repeatability in the calibration error (A-type uncertainty) and the B-type uncertainty contributions. The repeatability is calculated as in Sect. 4.1.2, while the B-type uncertainty contributions are described in the same section. Among these contributions, the uncertainty due to the chamber inhomogeneity between the radiosonde's sensor and the co-located reference thermometer has been estimated from the chamber inhomogeneity through the measurement volume, measured as the mean temperature difference between the two reference thermometers close to the radiosonde s' sensors, assuming the chamber homogeneity linearly dependent on the distance and considering the distances between the two reference thermometers (≈ 20 cm) and between each radiosonde's sensor and the co-located reference thermometer (≈ 3 cm).
The values of calibration errors and related uncertainties reported in Table 4 are also plotted in Fig. 11.

https://doi.org/10.5194/amt-2021-337
Preprint. Discussion started: 21 October 2021

T Rise (°C)	Before change				After change			
	Err_{cal}(RS41)	U[Err_{cal}(RS41)]	Err_{cal}(RS92)	U[Err_{cal}(RS92)]	Err_{cal}(RS41)	U[Err_{cal}(RS41)]	Err_{cal}(RS92)	U[Err_{cal}(RS92)]
"0+20"#1	0.14	0.05	-0.08	0.12	-0.10	0.08	0	0.13
"0+20"#3	-0.04	0.06	-0.21	0.11	0.17	0.13	-0.02	0.17
T Drop (°C)	**Before change**				**After change**			
	Err_{cal}(RS41)	U[Err_{cal}(RS41)]	Err_{cal}(RS92)	U[Err_{cal}(RS92)]	Err_{cal}(RS41)	U[Err_{cal}(RS41)]	Err_{cal}(RS92)	U[Err_{cal}(RS92)]
"20-5" #4	-0.10	0.05	0	0.09	-0.19	0.13	-0.22	0.27
"20-0" #2	0.17	0.04	-0.02	0.044	-0.11	0.10	-0.28	0.28

Table 4: Calibration error Err_{cal} and related uncertainty U(Err_{cal}) for RS41 and RS92 temperature sensors before and after the two rising changes from 0 °C to 20 °C (yellow rows) and the two dropping changes from 20 °C to 0 °C and -5 °C (gray rows). The numbers next to each temperature change in the left column indicate the time sequence of changes.

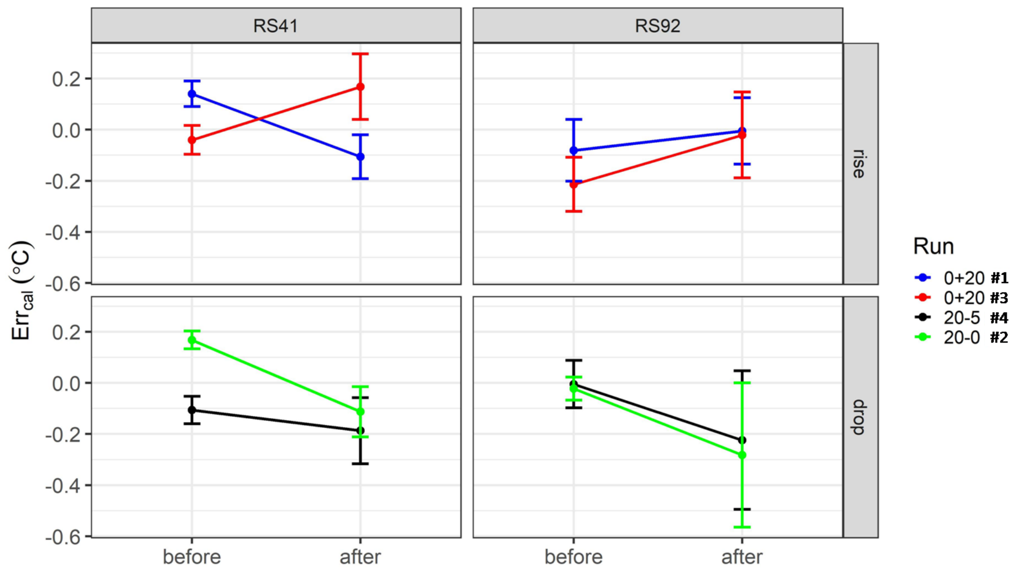

Figure 11: Plots of calibration errors Err_{cal} and related uncertainties (vertical bars) for RS41 and RS92 temperature sensors before and after the temperature changes (vertical axis). Top panels refer to rising changes, bottom panels to dropping changes, left panels to RS41 and right panels to RS92.

The results reported in Table 4 and plotted in Fig. 11 show how the calibration error of RS41 temperature sensor ranges from -0.1 °C to 0.2 °C before all the considered temperature changes and it does not change significantly after the changes, where it ranges from -0.2 °C to 0.2 °C. These values of calibration error for RS41 are slightly higher than those observed at the first stage of the experiment, where the corresponding calibration error was less than 0.1 °C in absolute value. For the temperature sensor of RS92, the calibration error is negative (cold bias), with absolute value less than 0.2 °C before all the changes and less than 0.3 °C after all the changes. Therefore, also for RS92 the temperature changes considered in this experiment do not significantly change the calibration error, which assumes values similar to those observed at the first stage of the experiment.

https://doi.org/10.5194/amt-2021-337
Preprint. Discussion started: 21 October 2021

The calibration uncertainties of RS41 and RS92 temperature sensors before and after each temperature change are very similar to their respective noises reported in Table 4, being their values less than 0.06 °C before the changes and less than 0.1 °C after the changes for RS41, less than 0.1 °C before the changes and ranging from 0.1 °C up to 0.3 °C after the changes for RS92. The above results indicate that a fast thermal change in the order of ±20 °C, that a radiosonde may meet before launch, does not appear to significantly affect the calibration error of temperature measurements collected after that change, but may lead to the increased calibration uncertainty observed in laboratory, due to the increase of sensor noise.

4.2.3 RS41 and RS92 temperature bias and uncertainty

The values of temperature absolute bias between RS92 and RS41, ΔT_{abs} (RS92, RS41), and of the related uncertainty, U [ΔT_{abs} (RS92, RS41)], before and after each of the temperature changes considered in the previous sections are reported in Table 5. ΔT_{abs} (RS92, RS41) is measured as difference between the calibration errors reported in Sect. 4.2.2, while its uncertainty is evaluated by combining in quadrature the corresponding calibration uncertainties. The same values reported in Table 5 are also plotted in Fig. 12.

T Rise (°C)	Before change		After change	
	ΔT_{abs}(RS92, RS41)	**U[ΔT_{abs}(RS92, RS41)]**	**ΔT_{abs}(RS92, RS41)**	**U[ΔT_{abs}(RS92,RS41)]**
"0+20"#1	-0.22	0.13	0.10	0.16
"0+20"#3	-0.17	0.12	-0.19	0.21
T Drop (°C)	Before change		After change	
	ΔT_{abs}(RS92, RS41)	**U[ΔT_{abs}(RS92, RS41)]**	**ΔT_{abs}(RS92, RS41)**	**U[ΔT_{abs}(RS92,RS41)]**
"20-5" #4	0.10	0.11	-0.03	0.30
"20-0" #2	-0.19	0.06	-0.17	0.30

Table 5: Temperature absolute bias between RS92 and RS41, ΔT_{abs} (RS92, RS41), and related uncertainty, U [ΔT_{abs} (RS92, RS41)], before and after the two rising changes from 0 °C to 20 °C (yellow rows) and the two dropping changes from 20 °C to 0 °C and -5 °C (gray rows). The numbers next to each temperature change in the left column indicate the time sequence of changes.

https://doi.org/10.5194/amt-2021-337
Preprint. Discussion started: 21 October 2021

Atmospheric Measurement Techniques Discussions

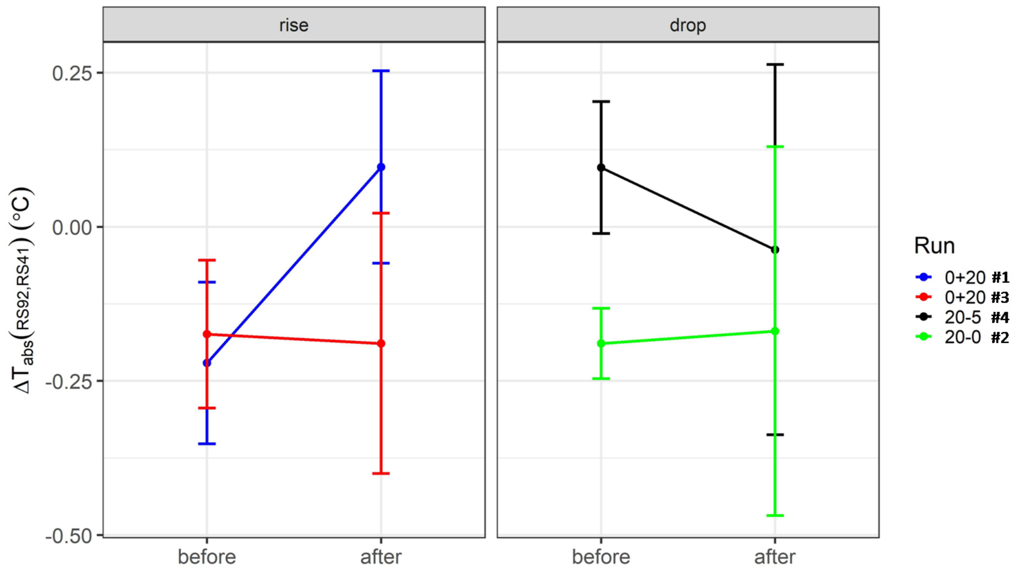

Figure 12: Plots of temperature absolute bias between RS92 and RS41, ΔT_{abs} (RS92, RS41), and related uncertainty (vertical bars) before and after the temperature changes (vertical axis). The left panel refers to rising changes, the right panel to dropping changes.

The results reported in Table 5 and plotted in Fig. 12 show that ΔT_{abs} (RS92, RS41) does not change significantly as a result of the temperature changes, with values ranging from -0.2 °C to 0.1 °C both before and after the changes. These values of temperature bias are similar to those observed at the first stage of the experiment under similar temperature conditions (see Fig. 9), where the corresponding bias was negative (RS92 colder than RS41) and less than 0.15°C in absolute value. The bias uncertainty U [ΔT_{abs} (RS92, RS41)] increases as a result of the temperature changes, being its values within 0.1°C before changes and ranging from 0.2°C to 0.3°C after changes. The above results indicate that fast thermal changes in the order of ±20 °C met by radiosondes before launch do not appear to affect the temperature bias between RS92 and RS41, but may lead to the increased bias uncertainty observed in laboratory, due to the increase of sensors' noise.

5 Summary and conclusions

Simultaneous comparisons between RS92 and RS41 radiosondes in climatic chambers have been performed for the first time independently of the manufacturer with the aim to characterize the noise, the calibration accuracy and the bias in temperature measurements. At a first stage of the experiment, radiosondes' performances were compared at ambient pressure and different temperature and humidity conditions, reproducing those that radiosondes meet at the ground and different latitudes and seasons. The data analysis revealed the following results:

- The temperature sensor of RS41 is less noisy than that of RS92, with noise values less than 0.06 °C for RS41 and within 0.1 °C for RS92.

- The calibration accuracy for RS41 temperature measurements is better than for RS92, with an absolute value of RS41 calibration error less than 0.1 °C and a calibration uncertainty (k = 1) less than 0.06 °C, while RS92 is affected by a cold bias in the calibration, which ranges from 0.1 °C up to a few tenths of a degree, with a calibration uncertainty less than 0.1 °C and 0.025 °C larger than that provided by the manufacturer. The lower calibration uncertainty for RS41 compared to RS92 is due to the lower noise of RS41. These results confirm the better performance of RS41 compared to RS92, in terms of both higher accuracy in pre-launch temperature measurements and simpler pre-launch ground check procedures.

- Under similar conditions that radiosondes meet in nighttime dual soundings at the ground, it is found that the temperature bias between RS41 and RS92 is within ±0.1 °C, with an uncertainty (k = 1) less than 0.1 °C. These values are in agreement with those reported in literature for nighttime dual soundings, both at near surface and throughout the troposphere, and suggest the possibility to integrate laboratory and dual soundings measurements for managing sensor changes within observing networks.

At a second stage of the experiment, RS41 and RS92 radiosondes were tested before and after fast (≈ 10 s) temperature changes of about ±20 °C, simulating steep thermal changes that radiosondes may meet when passing from indoor to outdoor conditions during the pre-launch phase. The data analysis revealed that these thermal changes may increase the noise of temperature measurements collected during radiosoundings, with noise values up to 0.1 °C for the RS41 and up to 0.3 °C for the RS92. This noise increase leads to a similar increase in the calibration uncertainty of radiosondes' temperature sensors, as well as an increase in the uncertainty of their bias up to 0.3 °C. On the other hand, the thermal changes do not appear to affect the calibration error and the bias of radiosondes' temperature measurements.

The results reported in this paper refer only to a specific pair of RS41 and RS92 radiosondes and they should be consolidated by further laboratory tests with multiple pairs of radiosondes. The methodology and the experimental setup used in this study can also be applied and adapted to characterize RS41 and RS92 humidity sensors, using reference hygrometers instead of the reference thermometers, as well as to characterize the sensors of other radiosonde models. Finally, it appears clear that further experiments in climatic chambers will be needed in the future to corroborate the results obtained from the analysis of radiosondes' intercomparisons and dual soundings' datasets. The overall goal of this analysis is to evaluate within a level of known uncertainty the effect of radiosondes models' change in climate data series, which is one of the goals of the WMO efforts in facing technology improvements and instrument changes.

Data availability. The measurement data from which the results in the figures and tables of this manuscript were obtained can be provided by the corresponding authors upon request

Author contribution. MR prepared the manuscript and contributed to the development of the experimental setup, as well as to the data collection and analysis. GC contributed to the manuscript writing and review, to the development of the experimental setup, and to the data collection and analysis. CM contributed to the manuscript review and the data collection and analysis. AM and FM provided scientific support through the experiment conceptualization, the applied methodology and the manuscript review.

Competing interests. The authors declare that they have no conflict of interest.

Acknowledgements. The authors wish to thank the GRUAN Lead Centre for providing a Vaisala MW41sounding system, the UHF antenna and the splitter, which allowed the simultaneous acquisition of measurements from RS92 and RS41.

https://doi.org/10.5194/amt-2021-337
Preprint. Discussion started: 21 October 2021

References

Bodeker, G. E., Bojinski, S., Cimini, D., Dirksen, R. J., Haeffelin,M., Hannigan, J. W., Hurst, D. F., Leblanc, T., Madonna, F., Maturilli, M., Mikalsen, A. C., Philipona, R., Reale, T., Seidel, D. J., Tan, D. G. H., Thorne, P. W., Vomel, H., and Wang, J.: Reference upper-air observations for climate: From concept to reality, B. Am. Meteorol. Soc., 97, 123–135, doi:10.1175/BAMS-D-14-00072.1, 2016.

Dirksen, R. J., Sommer, M., Immler, F. J., Hurst, D. F., Kivi, R., and Vömel, H.: Reference quality upper-air measurements: GRUAN data processing for the Vaisala RS92 radiosonde, Atmos. Meas. Tech., 7, 4463–4490, doi:10.5194/amt-7-4463-2014, 2014.

Dirksen, R. J., Bodeker, G. E., Thorne, P. W., Merlone, A., Reale, T., Wang, J., Hurst, D. F., Demoz, B. B., Gardiner, T. D., Ingleby, B., Sommer, M., von Rohden, C., and Leblanc, T.: Managing the transition from Vaisala RS92 to RS41 radiosondes within the Global Climate Observing System Reference Upper-Air Network (GRUAN): a progress report, Geosci. Instrum. Method. Data Syst., 9, 337–355, https://doi.org/10.5194/gi-9-337-2020, 2020.

Finazzi, F., Fassò, A., Madonna, F., Negri, I., Sun, B., and Rosoldi, M.: Statistical harmonization and uncertainty assessment in the comparison of satellite and radiosonde climate variables, Environmetrics 30 (2), e2528, 2019.

Free, M., Seidel, D. J., Angell, J. K., Lanzante, J., Durre, I., and Peterson, T. C.: Radiosonde Atmospheric Temperature Products for Assessing Climate (RATPAC): A new data set of large-area anomaly time series, J. Geophys. Res.-Atmos., 110, doi:10.1029/2005JD006169, 2005.

Gaffen, D. J.: Temporal inhomogeneities in radiosonde temperature records, J. Geophys. Res., 99, 3667–3676, 1994.

Gaffen, D. J., Sargent, M., Habermann, R. E., and Lanzante, J. R.: Sensitivity of tropospheric and stratospheric temperature trends to radiosonde data quality, J. Clim., 13, 1776– 1796, https://doi.org/10.1175/1520-0442(2000)013<1776:SOTAST>2.0.CO;2, 2000.

Haimberger, L., Tavolato, C., and Sperka, S.: Toward Elimination of the Warm Bias in Historic Radiosonde Temperature Records—Some New Results from a Comprehensive Intercomparison of Upper-Air Data, J. Climate, 21, 4587–4606, https://doi.org/10.1175/2008JCLI1929.1, 2008.

Haimberger, L., Tavolato, C., and Sperka, S.: Homogenization of the Global Radiosonde Temperature Dataset through Combined Comparison with Reanalysis Background Series and Neighboring Stations. J. Climate, *25*, 8108–8131, https://doi.org/10.1175/JCLI-D-11-00668.1, 2012.

Hersbach et al.: Operational global reanalysis: progress, future directions and synergies with NWP, ERA Report Series, 12/2018, 27, https://www.ecmwf.int/node/18765, 2018.

Hersbach, H., Bell, B., Berrisford, P., et al.: The ERA5 Global Reanalysis, QJR Meteorol Soc., 146:1999-2049, https://doi.org/10.1002/qj.3803, 2020.

Immler, F., Miloshevich, L., and GRUAN Task Team on radiosondes: Pre-launch Procedures for Vaisala RS92 Radiosonde Observations for GRUAN, Technical Document GRUAN-TD-5, https://gruan.files.wordpress.com/2011/06/gruan-td-5_rs92-pre-launch_v022.pdf, last access: 20 August 2021, 2011.

Jauhiainen, H., Survo, P., Lehtinen, R., and Lentonen, J.: Radiosonde RS41 and RS92 key differences and comparison test results in different locations and climates, TECO-2014, WMO Technical Conference on Meteorological and Environmental Instrumentsand Methods of Observations, Saint Petersberg, Russian Federation, 7–9 July 2014, P3(16), 2014.

Jensen, M. P., Holdridge, D. J., Survo, P., Lehtinen, R., Baxter, S., Toto, T., and Johnson, K. L.: Comparison of Vaisala radiosondes RS41 and RS92 at the ARM Southern Great Plains site, Atmos. Meas. Tech., 9, 3115–3129, https://doi.org/10.5194/amt-9-3115-2016, 2016.

https://doi.org/10.5194/amt-2021-337
Preprint. Discussion started: 21 October 2021

Jing, X., Shao, X., Liu, T.-C., and Zhang, B.: Comparison of GRUAN RS92 and RS41 Radiosonde Temperature Biases, Atmosphere, 12 (7), 857, https://doi.org/10.3390/atmos12070857, 2021.

Kawai, Y., Katsumata, M., Oshima, K., Hori, M. E., and Inoue, J.: Comparison of Vaisala radiosondes RS41 and RS92 launched over the oceans from the Arctic to the tropics, Atmos. Meas. Tech., 10, 2485-2498, https://doi.org/10.5194/amt-10-2485-2017, 2017.

Lanzante, J. R.: Resistant, robust and non-parametric techniques for the analysis of climate data: Theory and examples, including applications to historical radiosonde station data, Int. J. Climatol., 16, 1197–1226, https://doi.org/10.1002/(SICI)1097-0088(199611)16:11<1197::AID-JOC89>3.0.CO;2-L, 1996.

Loew, A., et al.: Validation practices for satellite-based Earth observation data across communities, Rev. Geophys., 55, 779–817, doi:10.1002/2017RG000562, 2017.

Madonna, F., Amodeo, A., Boselli, A., Cornacchia, C., Cuomo, V., D'Amico, G., Giunta, A., Mona, L., and Pappalardo, G.: CIAO: the CNR-IMAA advanced observatory for atmospheric research, Atmos. Meas. Tech., 4, 1191–1208, https://doi.org/10.5194/amt-4-1191-2011, 2011a.

Madonna, F., Burlizzi, P., Giunta, A., Binietoglou, I., Perrone, M. R., and Pappalardo, G.: Validation of COSMIC water vapor profiles using Raman lidar measurements performed at CIAO, Proceedings Volume 8182, Lidar Technologies, Techniques, and Measurements for Atmospheric Remote Sensing VII, 81820B, https://doi.org/10.1117/12.898117, 2011b.

Madonna, F., Rosoldi, M., Güldner, J., Haefele, A., Kivi, R., Cadeddu, M. P., Sisterson, D., and Pappalardo, G.: Quantifying the value of redundant measurements at GCOS Reference Upper-Air Network sites, Atmos. Meas. Tech., 7, 3813-3823, doi:10.5194/amt-7-3813-2014, 2014.

Madonna, F., Kivi, R., Dupont, J.-C., Ingleby, B., Fujiwara, M., Romanens, G., Hernandez, M., Calbet, X., Rosoldi, M., Giunta, A., Karppinen, T., Iwabuchi, M., Hoshino, S., von Rohden, C., and Thorne, P. W.: Use of automatic radiosonde launchers to measure temperature and humidity profiles from the GRUAN perspective, Atmos. Meas. Tech., 13, 3621–3649, https://doi.org/10.5194/amt-13-3621-2020, 2020.

Madonna, F., Summa, D., Di Girolamo, P., Marra, F., Wang, Y., and Rosoldi, M.: Assessment of Trends and Uncertainties in the Atmospheric Boundary Layer Height Estimated Using Radiosounding Observations over Europe, Atmosphere , 12(3), 301, https://doi.org/10.3390/atmos12030301, 2021a.

Madonna, F., Tramutola, E., SY, S., Serva, F., Proto, M., Rosoldi, M., Amato, F., Marra, F., Gagliardi, S., Fassò, A., Gardiner,T., and Thorne, P. W.: The new Radiosounding HARMonization (RHARM) dataset of homogenized radiosounding temperature, humidity and wind profiles with uncertainties. Part I: dataset description and characterization, Earth and Space Science Open Archive, 47, https://doi.org/10.1002/essoar.10507025.1, 2021b.

McCarthy, M.P.: Spatial sampling requirements for monitoring upper-air climate change with radiosondes, Int. J. Climatol., 28, 985–993, https://doi.org/10.1002/joc.1611, 2008.

McCarthy, M. P., Thorne, P. W., and Titchner, H. A.: An analysis of tropospheric humidity trends from radiosondes, J. Climate, 22, 5820–5838, doi:10.1175/2009JCLI2879.1, 2009.

Merlone, A., Lopardo, G., Sanna, F., Bell, S., Benyon, R., Bergerud, R., Bertiglia, F., Bojkovski, J., Böse, N., Brunet, M., Cappella, A., Coppa, G., del Campo, D., Dobre, M., Drnovsek, J., Ebert, V., Emardson, R., Fernicola, V., Flakiewicz, K., Gardiner, T., Garcia-Izquierdo, C., Georgin, E., Gilabert, A., Grykałowska, A., Grudniewicz, E., Heinonen, M., Holmsten, M., Hudoklin, D., Johansson, J., Kajastie, H., Kaykısızlı, H., Klason, P., Kňazovická, L., Lakka, A., Kowal, A., Müller, H., Musacchio, C., Nwaboh, J., Pavlasek, P., Piccato, A., Pitre, L., de Podesta, M., Rasmussen, M., Sairanen, H., Smorgon, D., Sparasci, F., Strnad, R., Szmyrka- Grzebyk, A., and Underwood, R.,: The

MeteoMet project - metrology for meteorology: challenges and results, Meteorol. Appl., vol. 22, pp. 820–829, doi: 10.1002/met.1528, Dec. 2015.

Merlone, A., Sanna, F., Beges, G., Bell, S., Beltramino, G., Bojkovski, J., Brunet, M., del Campo, D., Castrillo, A., Chiodo, N., Colli, M., Coppa, G., Cuccaro, R., Dobre, M., Drnovsek, J., Ebert, V., Fernicola, V., Garcia-Benadí, A., Garcia-Izquierdo, C., Gardiner, T., Georgin, E., Gonzalez, A., Groselj, D., Heinonen, M., Hernandez, S., Högström, R., Hudoklin, D., Kalemci, M., Kowal, A., Lanza, L., Miao, P., Musacchio, C., Nielsen, J., Nogueras-Cervera, M., OguzAytekin, S., Pavlasek, P., de Podesta, M., Rasmussen, M. K., Del-Río-Fernández, J., Rosso, L., Sairanen, H., Salminen, J., Sestan, D., Šindelářová, L., Smorgon, D., Sparasci, F., Strnad, R., Underwood, R., Uytun, A., and Voldan, M.: The MeteoMet2 project—highlights and results, Meas. Sci. Technol., vol. 29, no. 2, p. 025802, doi: 10.1088/1361-6501/aa99fc, Feb. 2018.

Merlone, A., Al-Dashti, H., Faisal, N., Cerveny, R.S., AlSarmi, S., Bessemoulin, P., Brunet, M., Driouech, F., Khalatyan, Y., Peterson, T. C., Rahimzadeh, F., Trewin, B., Wahab, M. M. A., Yagan, S., Coppa, G.,.Smorgon, D., Musacchio, C., and Krahenbuhl, D., Temperature extreme records: World Meteorological Organization metrological and meteorological evaluation of the 54.0°C observations in Mitribah, Kuwait and Turbat, Pakistan in 2016/2017, Int. J. Climatol., vol. 39, no. 13, pp. 5154–5169, doi: 10.1002/joc.6132, 2019.

Mona, L., Cornacchia, C., D'Amico, G., Di Girolamo, P., Pappalardo, G., Pisani, G., Summa, D., Wang, X., and Cuomo, V.: Characterization of the variability of the humidity and cloud fields as observed from a cluster of ground-based lidar systems, Quarterly Journal of Royal Meteorology Society, 133: (S3) 257–271, 2007.

Nash J., Oakley, T., Vomel, H., and Wei LI.: WMO Intercomparison of High Quality Radiosonde 1060 Systems Yangjiang, China, 12 July - 3 August 2010, WMO Instruments and Observing Methods 1061 Report No. 107, 2011.

Parker, D. E., and Cox, D. I.: Toward a consistent global climatological rawinsonde database, Int. J. Climatol., 15, 473–496, 1995.

Philipona, R., Mears, C., Fujiwara, M., Jeannet, P., Thorne, P., Bodeker, G., et al.: Radiosondes show that after decades of cooling, the lower stratosphere is now warming, Journal of Geophysical Research: Atmospheres, 123(22), 12, 509–12, 522, https://doi.org/10.1029/2018JD028901, 2018.

Pougatchev, N., August, T., Calbet, X., Hultberg, T., Oduleye, O., Schlüssel, P., Stiller, B., Germain, K. St., and Bingham, G.: IASI temperature and water vapor retrievals – error assessment and validation, Atmos. Chem. Phys., 9, 6453-6458, https://doi.org/10.5194/acp-9-6453-2009, 2009.

Rapp, A. D., Kummerow, C. D., and Fowler, L.: Interactions between warm rain clouds and atmospheric preconditioning for deep convection in the tropics, J. Geophys. Res., 116, D23210, doi:10.1029/2011JD016143, 2011.

Rosoldi, M., Gumà Claramunt, P., Madonna, F., Amodeo, A., Binietoglou, I., D'Amico, G., Giunta, A., Mona, L., Papagiannopoulos, N., and Pappalardo, G.: Study of thin clouds at CNR-IMAA Atmospheric Observatory (CIAO), Ann. Geophys., 56, https://doi.org/10.4401/ag-6337, 2013.

Seidel, D. J., Ao, C. O., and Li, K.: Estimating climatological planetary boundary layer heights from radiosonde observations: Comparison of methods and uncertainty analysis, J. Geophys. Res., 115, D16113, doi:10.1029/2009JD013680, 2010.

Sherwood, S., Lanzante, J., and Meyer, C.: Radiosonde daytime biases and late 20th century warming. Science 309 (5740): 1556–1559, 2005.

Sherwood, S. C., Meyer, C. L., Allen, R. J., and Titchner, H. A.: Robust tropospheric warming revealed by iteratively homogenized radiosonde data, J. Climate, 21, 5336–5350, doi:10.1175/ 2008JCLI2320.1, 2008.

https://doi.org/10.5194/amt-2021-337
Preprint. Discussion started: 21 October 2021

Atmospheric Measurement Techniques
Discussions

Sherwood, S. C., and Nishant, N.: Atmospheric changes through 2012 as shown by iteratively homogenised radiosonde temperature and wind data (IUKv2), Env. Res. Lett., Vol. 10, 054007, 2015.

Sun, B., Reale, T., Schroeder, S., Pettey, M., and Smith, R.: On the Accuracy of Vaisala RS41 versus RS92 Upper-Air Temperature Observations, J. Atmos. Oceanic Technol., 36, 635–653, https://doi.org/10.1175/JTECH-D-18-0081.1, 2019.

Survo, P., Lehtinen, R., and Kauranen, J.: SI traceability of Vaisala Radiosonde RS41 sounding data – calibration and uncertainty analysis, TECO-2014, WMO Technical Conference on Meteorological and Environmental Instruments and Methods of Observations, St. Petersburg, Russian Federation, July 7th-9th 2014, P2(7), 2014.

SY, S., Madonna, F., Rosoldi, M., et al.: Sensitivity of trends to estimation methods and quantification of sub sampling effects in global radiosounding temperature and humidity time series, Int. J. Climatol., 1–23, https://doi.org/10.1002/joc.6827, 2020

Thorne, P. W., Brohan, P., Titchner, H. A., McCarthy, M. P., Sherwood, S. C., Peterson, T. C., Haimberger, L., Parker, D. E., Tett, S. F. B., Santer, B. D., Fereday, D. R., and Kennedy, J. J.: A quantification of uncertainties in historical tropical tropospheric temperature trends from radiosondes, J. Geophys. Res.-Atmos., 116, D12116, doi:10.1029/2010jd015487, 2011.

Thorne, P. W., Madonna, F., Schulz, J., Oakley, T., Ingleby, B., Rosoldi, M., Tramutola, E., Arola, A., Buschmann, M., Mikalsen, A. C., Davy, R., Voces, C., Kreher, K., De Maziere, M., and Pappalardo, G.: Making better sense of the mosaic of environmental measurement networks: a system-of-systems approach and quantitative assessment, Geosci. Instrum. Method. Data Syst., 6, 453–472, https://doi.org/10.5194/gi-6-453-2017, 2017.

Vaisala: Vaisala Ground Check Set GC25, Datasheet Ref. B210357EN-B, Vaisala, https://www.vaisala.com/en/search?k=gc25&items_per_page=20&countyAddresmqihz=, last access: 20 August 2021, 2008.

Vaisala: 2010-12 | Revised Solar Radiation Correction Table RSN2010 | T**,** Sounding data continuity website, https://www.vaisala.com/en/sounding-data-continuity, last access: 20 August 2021, 2010.

Vaisala: Vaisala Radiosonde RS92-SGP, Datasheet Ref. B210358EN-F, Vaisala, https://www.vaisala.com/sites/default/files/documents/RS92SGP-Datasheet-B210358EN-F-LOW.pdf, last access 20 August 2021, 2013

Vaisala: Comparison of Vaisala Radiosondes RS41 and RS92, White Paper Ref. B211317EN-B, Vaisala, https://www.vaisala.com/sites/default/files/documents/RS-Comparison-White-Paper-B211317EN.pdf, last access: 20 August 2021, 2014.

Vaisala: Vaisala Sounding Processing Subsystem SPS311G, Datasheet Ref. B210492EN-E, Vaisala, https://www.vaisala.com/sites/default/files/documents/WEA-MET-SPS311-Datasheet-B210492EN.pdf, last access: 20 August 2021, 2016.

Vaisala: Vaisala Radiosonde RS41 Measurement Performance, White Paper Ref. B211356EN-B, Vaisala, https://www.vaisala.com/sites/default/files/documents/WEA-MET-RS41-Performance-White-paper-B211356EN-B-LOW-v3.pdf , last access: 20 August 2021, 2017a.

Vaisala: Vaisala Ground Check Device RI41/RI41-B, Datasheet Ref. B211322EN-C, Vaisala, https://www.vaisala.com/sites/default/files/documents/RI41-Datasheet-B211322EN.pdf, last access: 20 August 2021, 2017b.

Vaisala: Vaisala DigiCORA Sounding System MW41, Datasheet Ref. B211221EN-F, Vaisala, https://www.vaisala.com/sites/default/files/documents/B211221EN-F-Brochure.pdf, last access: 20 August 2021, 2018.

https://doi.org/10.5194/amt-2021-337
Preprint. Discussion started: 21 October 2021

von Rohden, C., Sommer, M., Naebert, T., Motuz, V., and Dirksen, R. J.: Laboratory characterisation of the radiation temperature error of radiosondes and its application to the GRUAN data processing for the Vaisala RS41, Atmos. Meas. Tech. Discuss. [preprint], https://doi.org/10.5194/amt-2021-187, in review, 2021.

Whiteman, D. N., Melfi, S. H., and Ferrare, R. A.: Raman lidar system for the measurement of water vapor and aerosols in the Earth's atmosphere, Appl. Opt. 31(16), 3068–3082, 1992.

Zhou, D. K., Smith, W. L., Cuomo, V., Taylor, J. P., Barnet, C. D., Di Girolamo, P., Pappalardo, G., Larar, A. M., Liu, X., Newman, S. M., Lee, C., and Mango, S. A.: Retrieval validation during the European Aqua Thermodynamic Experiment, Q. J. Roy. Meteorol. Soc., 133, 203–215, 2007.